Anatomy of the long head of biceps femoris: an ultrasound study

D Tosovic[1], JC Muirhead[2], JMM Brown[1], SJ Woodley[2*].

[1]*Department of Anatomy & Developmental Biology, School of Biomedical Sciences, University of Queensland, Brisbane, Australia, 4072.*

[2]*Department of Anatomy, Otago School of Medical Sciences, University of Otago, Dunedin, New Zealand, 9016.*

*Correspondence to:

Stephanie Woodley

Department of Anatomy

University of Otago

PO Box 56

Dunedin

NEW ZEALAND

Email: stephanie.woodley@anatomy.otago.ac.nz

This article has been accepted for publication and undergone full peer review but has not been through the copyediting, typesetting, pagination and proofreading process which may lead to differences between this version and the Version of Record. Please cite this article as an 'Accepted Article', doi: 10.1002/ca.22718

Anatomy of the long head of biceps femoris: an ultrasound study

ABSTRACT

Introduction: Hamstring strains, particularly involving biceps femoris long head (BFlh) at the proximal musculotendinous junction (MTJ), are commonly experienced by athletes. With the use of diagnostic ultrasound increasing, an in-depth knowledge of normal ultrasonographic anatomy is fundamental to better understanding hamstring strain. This study aimed to describe the architecture of BFlh, using ultrasonography, in young men and cadaver specimens. **Materials and Methods:** BFlh morphology was examined in 19 healthy male participants (mean age 21.6 years) using ultrasound. Muscle, tendon and MTJ lengths were recorded and architectural parameters assessed at four standardised points along the muscle. Measurement accuracy was validated by ultrasound and dissection of BFlh in six male cadaver lower limbs (mean age 76 years). Intra-rater reliability of architectural parameters was examined for repeat scans, image analysis and dissection measurements. **Results:** Distally the BFlh muscle had significantly ($p<0.05$) shorter fascicles and larger pennation angles than proximal sites. Agreement between ultrasound and dissection (cadaver study) was excellent for all architectural parameters, except pennation angle (PA), and MTJ length. All other measures demonstrated good-excellent repeatability. **Conclusions:** BFlh is not uniform in architecture when imaged using ultrasound. It is likely that its distal most segment is better suited for force production in comparison to the more proximal segments, which show excursive potential, traits which possibly contribute to the high rate of injury at the proximal MTJ. The data presented in this study provide specific knowledge of the normal ultrasonographic anatomy of BFlh, which should be of assistance in analysing BFlh injury via imaging.

Key words: ultrasonography; muscle, skeletal; tendons

INTRODUCTION

Hamstring strains are one of the most common injuries sustained by athletes, particularly in sports involving dynamic muscle movements such as sprinting and kicking (Brockett et al., 2004; Proske et al., 2004; Hoskins and Pollard, 2005; Petersen et al., 2010; Eirale et al., 2013; Orchard et al., 2013). These injuries, which are often recurrent (Croisier et al., 2002; Verrall et al., 2006; Petersen et al., 2010; Eirale et al., 2013; Orchard et al., 2013), can result in long periods of exclusion from competitionand a delay in return to pre-injury levels of activity (Gibbs et al., 2004; Petersen et al., 2010; Eirale et al., 2013; Orchard et al., 2013). Several factors increase the likelihood of hamstring strains including their two-joint anatomy and their forceful activation during eccentric contractions (Mair et al., 1996; Thelen et al., 2005; Opar et al., 2012). Injuries to the long head of biceps femoris (BFlh) are of particular interest, as they constitute over 80% of all hamstring strains (Kouloris & Connell, 2003; Ekstrand et al., 2012), with most strains occurring proximally at the musculotendinous junction (MTJ) (De Smet and Best, 2000; Slider et al., 2008; Slider et al., 2010). The frequency and consequences of these injuries promote the need to understand the normal anatomy of the hamstring muscles so to enhance clinical assessment and rehabilitation.

Muscle architecture is an important factor in models of hamstring strain injury (Mendiguchia et al., 2011). A muscle may be composed of anatomical segments defined by unique architectural differences (e.g. fascicle length, fascicle orientation) throughout its length (Wickham and Brown, 1998; Sakoma et al., 2011;Tosovic et al., 2012). Several segments may be present within a muscle, each of which may differ in function and neuromuscular activation (Wickham et al., 2004) and thus possibly in their predisposition to injury. Morphological data pertaining to BFlh have been reported inseveral studies (Seidel et al., 1996; Woodley & Mercer, 2005; Makihara et al., 2006; Kellis et al., 2010; Lieber, 2010; van

der Made et al., 2013). However, few have focused on segmental architecture (Woodley and Mercer 2005; Kellis et al., 2010), and most data have been derived fromlinear measures in cadaver specimens. Ultrasound imaging is increasingly being used in the assessment of hamstring injuries (Kouloris & Connell, 2006; Petersen et al., 2014), and more recently this technique has been employed to investigate normal hamstring architecture (Blackburn et al., 2009; Kellis et al., 2010; Abe et al., 2014; Blackburn and Pamukoff, 2014; e Lima et al., 2015; Palmer et al., 2015). However, with the exception of one cadaver study (Kellis et al., 2010), sonographic research has largely been directed towards obtaining whole muscle measurements rather than examining potential architectural variations that may be evident throughout the length of BFlh. Therefore, determining the morphology of BFlh with ultrasound in a healthy population, particularly the anatomy of its segments, may contribute to a better understanding of hamstring strain, aid with interpreting images of hamstring injury, and so facilitate rehabilitation.

The principle aim of this study was to document the ultrasonographic anatomy of BFlh in young healthy men, and to determine whether it is possible to distinguish individual segments within the muscle. Secondary objectives were to validate the sonographic measurements using cadaver specimens and to provide information on the repeatability of the sonographic and dissection measures.

MATERIALS AND METHODS

Healthy Volunteer Study

Participants

Twenty physically active males (Pate et al., 1995) aged 18-30 years old (mean age, 21.6±2.3 years; mean BMI, 24.7±2.6kg/m^2) were recruited from the local community. Participants were excluded if they had a history of posterior thigh injury (acute or chronic) or any systemic musculoskeletal disorder. Ethical approval was granted by the University Human Ethics Committee (reference: 13/084) and written informed consent was obtained.

Ultrasound Imaging

Ultrasound scans were performed by an experienced sonographer (JM) using a Siemens Sonoline Antares^{TM} ultrasound machine (Siemens Medical Solutions USA, Inc., Malvern, PA) with a VF10-5 line array probe (5-10 MHz; Siemens). Extended field-of-view technology was utilised to capture images that encapsulated the full length of muscle fascicles. Participants were positioned prone with their lower limbs extended in neutral rotation and scanned bilaterally.

The insertion sites of BFlh at the ischial tuberosity (proximally) and the head of the fibula (distally), along with the most proximal and distal extents of muscle fibre insertion onto the proximal and distal tendons respectively, were scanned and the position of each was marked on the skin. Using these skin markings the following lengths were recorded with a flexible tape measure: total muscle-tendon, total muscle (ML; exclusive of distal free tendon), proximal musculotendinous junction (MTJ) (incorporating the proximal free tendon, as it was not possible to isolate and measure this structure due to its short length), distal MTJ and distal free tendon (devoid of any muscle fibre insertion) (Woodley and Mercer, 2005; Askling et

al., 2007). Additional scans were then taken systematically, at four points along BFlh, namely at 30%, 50%, 70% and 90% of the total muscle length (Kellis et al., 2009), to examine muscle thickness (MT), fascicle length (FL) and pennation angle (PA). With the ultrasound probe oriented in the transverse plane, MT was measured at the time of scanning and was defined as the vertical length between the superficial and deep aponeuroses at each measurement site (Kellis et al., 2009) (Figure 1A). Still ultrasound images were also taken with the probe aligned along the long axis of BFlh, and these images were imported as DICOM files into ImageJ (National Institutes of Health, Bethesda, Maryland, USA) for analysis of FL and PA (undertaken by DT) (Figure 1B). Fascicle length (mm) was defined as the length of an entire muscle fascicle that extended from the superficial aponeurosis to the deep intramuscular aponeurosis and was calculated by setting the appropriate scale and using the 'straight line tool'. Pennation angle (^{o}) was defined as the angle between the superficial aponeurosis and a clearly visible fascicle, measured using the 'angle tool' (Kawakami et al., 1993).

Intra-observer Reliability

To assess reliability, both limbs from five participants were rescanned after a period of at least three days (JM) at each of the four predetermined regions, and all architectural parameters were remeasured. In addition, repeat measurements of FL and PA from still ultrasound images of both limbs from five randomly selected participants were performed (DT). The investigators were blinded to their original measurements for both procedures.

INSERT FIGURE 1 HERE

Cadaver Validation Study

Specimens

The BFlh was investigated in six lower limbs from three embalmed male cadavers (mean age at death 76 years, range 65-86 years) bequeathed to the Department of Anatomy, University of Otago under the New Zealand Human Tissue Act (2008), using a combination of ultrasound and dissection.

Ultrasound Imaging

The same ultrasound protocol was used as for the healthy volunteer study, with the exception that following the scans at 30%, 50%, 70% and 90% of muscle length, pins were inserted into the muscle at each point, so to serve as reference for the dissection phase.

Dissection

The skin, superficial and deep fascia of the gluteal region and posterior thigh, and the gluteus maximus muscle were resected, taking care not to disturbthe pins. As for the healthy volunteer study, a flexible tape measure was utilised to measure larger parameters such as ML, proximal and distal MTJ lengths, as well as distal free tendon length. At each pinned region of BFlh, MT (mm) was recorded using electronic calipers (Tresna, point digital sliding calipers SC02, Germany). The muscle was then sectioned longitudinally in order to measure FL (calipers) (Figure 2) and PA using a standard protractor. These parameters were measured at the point that the pin penetrated the superficial aponeurosis.

INSERT FIGURE 2 HERE

Intra-observer Reliability

Measures pertaining to all architectural parameters except PA and FLwere measured a second time; at least four days apart, for four of the six specimens.

Statistical Analyses

Data were exported to a Microsoft Excel spreadsheet and means and standard deviations of all morphometric parameters calculated, and where relevant, mean values were calculated for the BFLh as a whole (cadaver study n=6; healthy volunteer study n=19). Fascicle length/muscle length (FL/ML) ratio was calculated by dividing the mean fascicle length determined for each scan site by muscle length (Lieber, 2010). One-way analysis of variance (ANOVA; GraphPad Prism software) was used to assess for statistically significant differences between the four scan points for measures of FL, PA, MT and FL/ML ratio in the living participants. A p-value of <0.05 was considered statistically significant.

Intraclass correlation coefficients (ICC) were calculated and analysed using the criteria of Landis and Koch (1977) to compare the reliability of (a) measures obtained from repeat scans as well as (b) the intra-observer reliability of measurements taken from the still ultrasound scans (healthy volunteer study) and (c) measurements obtained from ultrasound and dissection (cadaver study). For the latter, recordings from all four respective measurement sites were pooled to calculate ICC values. Additionally, architectural measurements obtained via ultrasound from both the healthy volunteers and cadavers were compared using unpaired student t-tests (GraphPad Prism software).

RESULTS

Healthy Volunteer Study

Muscle architecture

The results obtained from 19 healthy male volunteers using ultrasound are presented in Table 1. Data from one participant were excluded due to poor image quality.

INSERT TABLE 1 HERE

The proximal BFlh (30% ML) had a significantly smaller pennation angle than the three other measurement sites (P<0.05). Conversely, the distal part of BFlh (90%ML) had significantly shorter fascicles than the other measurement sites (P<0.05). The two middle portions of BFlh (50% and 70% ML) were significantly thicker than each of the peripheries, whilst the most distal site was significantly thinner than the rest (P<0.05). Similar to FL, the distal part of BFlh (90% ML) had a significantly smaller FL/ML ratio than the other measurement sites. The proximal MTJ extended over 76.9% of the total muscle length of BFlh, whilst the distal MTJ extended over 49.76% of the total muscle length. The overlap of the two MTJs was contained within approximately 27% of the ML.

Intra-observer Reliability

Intra-observer reliability for the measurements taken from repeat scans was excellent for most architectural parameters (ICC: PA 0.81, proximal MTJ length 0.81, FL 0.91, MT 0.92, distal MTJ length 0.93, ML 0.93), with the exception of distal free tendon length (very good; ICC 0.71) and total muscle-tendon length (very good; ICC 0.73). Similarly reanalyses of the ultrasound images showed excellent reliability for both fascicle length (ICC 0.97) and pennation angle (ICC 0.97).

Cadaver Validation

Architectural data from dissection and ultrasound of the six cadaver specimens are presented in Table 2. An excellent level of agreement between the two methods of measurement was observed for the majority of measurements with the exception of proximal MTJ length (average) and distal MTJ length and PA (poor).

INSERT TABLE 2 HERE

Intra-observer Repeatability

Intra-observer repeatability for repeat measurements of muscle architecture obtained from the cadavers was excellent for most measures, (ICC: distal MTJ length 0.95, ML 0.97, proximal MTJ length 0.97, total muscle-tendon length 0.99, MT 0.99), with the exception of distal free tendon length, which was very good (ICC 0.78).

Comparison between ultrasound data obtained from healthy volunteers and cadavers showed that PA, MT, ML, proximal MTJ length and distal MTJ length were significantly *(P*<0.05) larger in the healthy participants. No significant difference was found between total muscle-tendon length and FL, whilst distal free tendon length was significantly *(P*<0.05) longer in the cadavers (Table 3).

INSERT TABLE 3 HERE

DISCUSSION

In young healthy men, architecture was variable throughout the length of BFlh. Of note the distal most part of the muscle (90% ML) contained shorter fascicles which were more pennated than its proximal most site (30% ML). This arrangement is typical of muscles designed for force production, where the pennated orientation allows for a relatively greater number of fascicles to be packed in the muscle, parallel to each other (Wickiewicz et al., 1983; Aagaard et al., 2001). Thus, it appears that the proximal segment of BFlh has larger excursive potential (FL/ML ratio = 0.25) compared to its distal region (90% ML; FL/ML ratio = 0.22) (Table 1), which appears better suited to force generation. A three-dimensional muscle model created by Rehorn and Blemker (2010) demonstrates that non-uniform stretching occurs within BFlh, with the largest degree of muscle stretch localised near the proximal MTJ during activated muscle lengthening (eccentric contractions). The results of our study compliment these findings as the two most proximal segments with the largest fascicle lengths, would theoretically have the highest excursive potential (FL/ML ratio = 0.25 and 0.26, respectively) (Table 1).

Perhaps the fundamental difference in proximal and distal muscle architecture may contribute to understanding why the majority of BFlh strains occur at the proximal MTJ (De Smet and Best, 2000; Slider et al., 2008). Pennated muscles are able to utilise the length-tension curve more effectively as they have the ability to produce a larger amount of force over a smaller range of motion (Astrand et al., 1986). Consequently, their length-tension curve is narrower, indicating that applying the same length of stretch to a pennate muscle as a parallel-fibred muscle would be more detrimental to force production over greater lengths. However, the findings from Rehorn and Blemker (2010) would suggest that this detrimental effect on force production would not affect the distal portion of BFlh as significantly, as the lengthening

experienced distally is not as great as that at the proximal MTJ. Therefore, it appears that the distal segment is better equipped to avoid the lengthening that occurs at the proximal most segment. Furthermore, Garrett et al (1988) investigated muscles of various architectures to determine the degree of elongation, relative to resting fibre length that was required to reach failure point (rupture). Their results showed that pennated muscles had the ability to elongate to a greater degree before experiencing ruptures. Given that the proximal segment of BFlh was found to have longer fascicle lengths and smaller pennation angles, it may possess a reduced capacity to elongate/adjust to changes in length, in turn meaning that this architecture may contribute in some part to the high rate of strains experienced at the proximal MTJ.

Muscle thickness is a good indicator of muscle size and cross-sectional area (Takai et al., 2011), both of which are related to the force producing capacity of a muscle (Wickiewicz et al., 1983; Lieber and Friden, 2000). In this study the two middle-most sites were found to be significantly thicker than both peripheries, a morphology expected from a fusiform shaped muscle (Sanchez et al., 2006). Thus, the sheer size of these two segments could result in them being able to contribute the greatest amount of the force generated by the muscle, irrespective of their fascicular orientation.

In general, ultrasound measures of mean BFlh MT, total muscle-tendon length and PA from the healthy male participants in our study were similar to previous reports (Chelboun et al., 2001; Blackburn et al., 2009; 2014; e Lima et al., 2015; Palmer et al., 2015). Although MT measures were found to be within the range reported in two recent studies (22.7±4 mm - 36.6±4.9mm), there appears to be large discrepancy between these reports (e Lima et al., 2015; Palmer et al., 2015). This variability may relate to the difference in the size of the

respective participant groups, with BMI values ranging from 24.44kg/m^{2}to 26.15kg/m$^{2.}$. Similar to MT measures, the mean BMI of participants from our study (24.7±2.6kg/m^2) was within the range of the aforementioned reports. FL measures (77.9±14mm) were similar to those documented by e Lima et al (2015) (87.7±10.2mm), although substantially shorter than reported by both Chelboun et al (2001) (~110mm) and Blackburn et al (2014) (141±45mm). Differences may be attributed to methods of measuring captured images, with one study relying upon extrapolation of fascicles to estimate length (Blackburn et al., 2014), and the other piecing together a montage of a series of images (Chelboun et al., 2001). In this study we were able to determine FL using extended field-of-view technology which allowed panoramic images of longer fascicles to be captured, encapsulating their full length.

To the best of our knowledge, this is the first study to document the normal anatomy throughout the length of the BFlh muscle in healthy living participants, meaning direct comparison to other studies is limited. However, when compared with the work of Kellis et al (2010), who similarly investigated four sites along BFlh (in cadavers), we find agreement around longer fascicles being confined to the proximal part of the muscle. This finding was also supported by the segmental ultrasound data from our cadaver specimens (in relative but not absolute terms), whereby the most proximal site displayed the largest mean FL. Contrary results were observed for PA and MT. Kellis et al (2010) reported the proximal section to be the thickest (with the largest PA), with dimensions progressively reducing at the subsequent distal sites, whereas data from both our healthy individuals and cadaver specimens demonstrated that the most proximal part of BFlh had the smallest mean PA, while the two middle sites were the thickest. However, as smaller muscle volumes and cross-sectional areas are observed in aged cadavers (Kirkendall and Garrett, 1998; Lexell and Downham, 1992), these differing outcomes may be expected if a non-uniform loss of muscle tissue had

occurred. Interestingly, in our study MT in the cadaver specimens showed a similar trend to that of healthy participants, although the values were significantly smaller, indicating uniform muscle loss across the different sites investigated.

The apparent effects of ageing are further demonstrated by comparison of ultrasonographic data from young men and male cadavers. Most architectural parameters, including PA, MT, ML, and MTJ lengths were significantly smaller in the cadavers. As a consequence of decreased ML, distal free tendon length was in turn found to be significantly longer in cadavers. Interestingly, no significant difference was observed for FL between the two groups. However, this outcome perhaps clarifies why a smaller PA was observed in cadavers, as a reduced PA would be required to accommodate fascicles of the same length in a muscle which has become thinner (decreased MT).

Measurement reliability is an important factor when considering the potential clinical utility of any ultrasound protocol. As ultrasound is highly operator dependent (Bianchi et al., 2005), it is positive that good to excellent repeatability was established for the measurements recorded within this study (scans, image analysis and dissection). Similar reliability was evident when comparing ultrasound and dissection, with the exception of PA, and MTJ lengths which displayed a poor to average level of agreement. Unlike FL and MT, the results obtained for PA differ from previous studies which report excellent agreement (Kellis et al., 2009; Chelboun et al., 2001). However, the absolute mean difference in PA between ultrasound and dissection was small (2.7^{o}), and as the changes in PA across the muscle were also small, the error rate is likely to be higher than it would befor measures of larger architectural parameters such as FL. Different measurement methods may also influence repeatability, with values derived from computer-based analysis likely to be more accurate

than those taken using a standard protractor. The low level of agreement for measuring proximal and distal MTJ lengths was unexpected. It is possible that the two-dimensional nature of ultrasound contributed to difficulties in consistently detecting the tapering tendon endings within the muscle belly.

Limitations

The present study assessed intra-rater reliability, however as mentioned previously, ultrasound is reliant on the skills of the operator (Bianchi et al., 2005), so assessing inter-rater reliability would be of additional value to incorporate into future studies. Male participants and cadavers were included in this study given that men are most likely to sustain a hamstring strain (Cross et al., 2013), but it would be interesting to examine whether females demonstrate similar muscle-tendon architecture. Similarly, investigating the ultrasonographic anatomy of the hamstring complex as a whole is necessary to appreciate the relationship between BFlh and the other muscles in this group, given not all injuries are isolated to BFlh. Normalising the data in relation to body height would have optimised comparison of architectural data between the healthy volunteers and cadaver specimens. However, this was not possible as height data were unavailable for the cadavers. Taking this into consideration, it may be possible that the differences in muscle-tendon length measurements between the two groups could be attributed to potential differences in height, particularly given the relatively small sample size of the cadaver validation study.

Conclusions

Ultrasonographic investigation has revealed novel data which indicate that segments of the BFlh muscle are not uniform with respect to their architecture. The functional implications of the morphological differences observed between the most distal and more proximal segments

of BFlh may provide further insight into why the proximal MTJ is most predisposed to injury. Furthermore, this study provides a detailed account of the normal ultrasonographic anatomy of BFlh, which will be of assistance in analysing BFlh injury through imaging.

Acknowledgements

The authors would like to express their sincere gratitude to the donors and their families, and to the young men who participated in this study. This study was jointly funded by a grant received from the Otago School of Medical Sciences (University of Otago) and the School of Biomedical Sciences (University of Queensland).

REFERENCES

Aagaard P, Andersen JL, Dyhre-Poulsen P, Leffers AM, Wagner A, Magnusson SP, Halkjaer-Kristensen J, Simonsen EB. 2001. A mechanism for increased contractile strength of human pennate muscle in response to strength training: changes in muscle architecture. J Physiol 534:613-623.

Abe T, Loenneke JP, Thiebaud RS. 2014. Ultrasound assessment of hamstring muscle size using posterior thigh muscle thickness. Clin Physiol Funct Imaging Epub ahead of print DOI: 10.1111/cpf.12214.

Askling CM, Tengvar M, Saartok T, Thorstensson A. 2007. Acute first-time hamstring strains during slow-speed stretching: clinical, magnetic resonance imaging, and recovery characteristics. Am J Sports Med 35: 1716-1724.

Astrand P-O, Rodhal K. 1986. Textbook of Work Physiology. 3rd Ed. New York: McGraw-Hill.p64.

Bianchi S, Martinoli C, Abdelwahab IF. 2005. Ultrasound of tendon tears. Part 1: general considerations and upper extremity. Skeletal Radiol 34:500-512.

Blackburn JT, Bell DR, Norcross MF, Hudson JD, Kimsey MH. 2009. Sex comparison of hamstring structural and material properties. Clin Biomech 24:65-70.

Blackburn JT Pamukoff DN. 2014. Geometric and architectural contributions to hamstring musculotendinous stiffness. Clin Biomech 29:105-110.

Brockett CL, Morgan DL, Proske U. 2004. Predicting hamstring strain injury in elite athletes. Med Sci Sports Exerc 36:379-387.

Chleboun GS, France AR, Crill MT, Braddock HK, Howell JN. 2001. In vivo measurement of fascicle length and pennation angle of the human biceps femoris muscle. Cells Tissues Organs 169:401-409.

Croisier JL, Forthomme B, Namurois MH, Vanderthommen M, Crielaard JM. 2002. Hamstring muscle strain recurrence and strength performance disorders. Am J Sports Med 30:199-203.

Cross KM, Gurka KK, Saliba S, Conaway M, Hertel J. 2013. Comparison of hamstring strain injury rates between male and female intercollegiate soccer athletes. Am J Sports Med 41:742-748.

De Smet AA, Best TM. 2000. MR imaging of the distribution and location of acute hamstring injuries in athletes. AJR Am J Roentgenol174:393-399.

e Lima KM, Carneiro SP, Alves Dde S, Peixinho CC, de Oliveira LF. 2015. Assessment of muscle architecture of the biceps femoris and vastuslateralis by ultrasound after a chronic stretching program. Clin J Sport Med 25:55-60.

Eirale C, Farooq A, Smiley FA, Tol JL, Chalabi H. 2013. Epidemiology of football injuries in Asia: a prospective study in Qatar. J Sci Med Sport 16:113-117.

Ekstrand J, Healy JC, Walden M, Lee JC, English B, Hagglund M. 2012. Hamstring muscle injuries in professional football: the correlation of MRI findings with return to play. Br J Sports Med 46:112-117.

Garrett WE, Jr., Nikolaou PK, Ribbeck BM, Glisson RR, Seaber AV. 1988. The effect of muscle architecture on the biomechanical failure properties of skeletal muscle under passive extension. Am J Sports Med 16:7-12.

Gibbs NJ, Cross TM, Cameron M, Houang MT. 2004. The accuracy of MRI in predicting recovery and recurrence of acute grade one hamstring muscle strains within the same season in Australian Rules football players. J Sci Med Sport 7:248-258.

Hoskins WT, Pollard HP. 2005. Successful management of hamstring injuries in Australian Rules footballers: two case reports. Chiropr Osteopat 13:4.

Kawakami Y, Abe T, Fukunaga T. 1993. Muscle-fiber pennation angles are greater in hypertrophied than in normal muscles. J Appl Physiol 74:2740-2744.

Kellis E, Galanis N, Natsis K, Kapetanos G. 2009. Validity of architectural properties of the hamstring muscles: correlation of ultrasound findings with cadaveric dissection. J Biomech 42:2549-2554.

Kellis E, Galanis N, Natsis K, Kapetanos G. 2010. Muscle architecture variations along the human semitendinosus and biceps femoris (long head) length. J Electromyogr Kinesiol 20:1237-1243.

Kirkendall DT, Garrett WE, Jr. 1998. The effects of aging and training on skeletal muscle. Am J Sports Med 26:598-602.

Koulouris G, Connell D. 2003. Evaluation of the hamstring muscle complex following acute injury. Skeletal Radiol 32:582-589.

Koulouris G, Connell D. 2005. Hamstring muscle complex: an imaging review. Radiographics 25:571-586.

Landis JR, Koch GG. 1977. The measurement of observer agreement for categorical data. Biometrics 33:159-174.

Lexell J, Downham D. 1992. What is the effect of ageing on type 2 muscle fibres? J Neurol Sci 107:250-251.

Lieber RL, Friden J. 2000. Functional and clinical significance of skeletal muscle architecture. Muscle Nerve 23:1647-1666.

Lieber RL. 2010. Skeletal Muscle Structure, Function and Plasticity; the Physiological Basis of Rehabilitation. 3rd Ed. Philadelphia: Lippincott Wilkins &Williams. p 26.

Mair SD, Seaber AV, Glisson RR, Garrett WE, Jr. 1996. The role of fatigue in susceptibility to acute muscle strain injury. Am J Sports Med 24:137-143.

Makihara Y, Nishino A, Fukubayashi T, Kanamori A. 2006. Decrease of knee flexion torque in patients with ACL reconstruction: combined analysis of the architecture and function of the knee flexor muscles. Knee Surg Sports Traumatol Arthrosc 14:310-317.

Mendiguchia J, Alentorn-Geli E, Brughelli M. 2012. Hamstring strain injuries: are we heading in the right direction? Br J Sports Med 46:81-85.

Opar DA, Williams MD, Shield AJ. 2012. Hamstring strain injuries: factors that lead to injury and re-injury. Sports Med 42:209-226.

Orchard JW, Seward H, Orchard JJ. 2013. Results of 2 decades of injury surveillance and public release of data in the Australian Football League. Am J Sports Med 41:734-741.

Palmer TB, Akehi K, Thiele RM, Smith DB, Thompson BJ. 2015. Reliability of panoramic ultrasound imaging in simultaneously examining muscle size and quality of the hamstring muscles in young, healthy males and females. Ultrasound Med Biol 41:675-684.

Pate RR, Pratt M, Blair SN, Haskell WL, Macera CA, Bouchard C, Buchner D, Ettinger W, Heath GW, King AC, et al. 1995. Physical activity and public health. A recommendation from the Centers for Disease Control and Prevention and the American College of Sports Medicine. JAMA 273:402-407.

Petersen J, Thorborg K, Nielsen MB, Holmich P. 2010. Acute hamstring injuries in Danish elite football: a 12-month prospective registration study among 374 players. Scand J Med Sci Sports 20:588-592.

Petersen J, Thorborg K, Nielsen MB, Skjodt T, Bolvig L, Bang N, Holmich P. 2014. The diagnostic and prognostic value of ultrasonography in soccer players with acute hamstring injuries. Am J Sports Med 42:399-404.

Proske U, Morgan DL, Brockett CL, Percival P. 2004. Identifying athletes at risk of hamstring strains and how to protect them. Clin Exp Pharmacol Physiol 31:546-550.

Rehorn MR, Blemker SS. 2010. The effects of aponeurosis geometry on strain injury susceptibility explored with a 3D muscle model. J Biomech 43:2574-2581.

Sakoma Y, Sano H, Shinozaki N, Itoigawa Y, Yamamoto N, Ozaki T, Itoi E. 2011. Anatomical and functional segments of the deltoid muscle. J Anat 218:185-190.

Sanchez AR 2nd, Sugalski MT, LaPrade RF. 2006. Anatomy and biomechanics of the lateral side of the knee. Sports Med Arthrosc 14:2-11.

Seidel PM, Seidel GK, Gans BM, Dijkers M. 1996. Precise localization of the motor nerve branches to the hamstring muscles: an aid to the conduct of neurolytic procedures. Arch Phys Med Rehabil 77:1157-1160.

Silder A, Heiderscheit BC, Thelen DG, Enright T, Tuite MJ. 2008. MR observations of long-term musculotendon remodelling following a hamstring strain injury. Skeletal Radiol 37:1101-1109.

Silder A, Reeder SB, Thelen DG. 2010. The influence of prior hamstring injury on lengthening muscle tissue mechanics. J Biomech 26:2254-2260.

Takai Y, Katsumata Y, Kawakami Y, Kanehisa H, Fukunaga T. 2011. Ultrasound method for estimating the cross-sectional area of the psoas major muscle. Med Sci Sports Exerc 43:2000-2004.

Thelen DG, Chumanov ES, Hoerth DM, Best TM, Swanson SC, Li L, Young M, Heiderscheit BC. 2005. Hamstring muscle kinematics during treadmill sprinting. Med Sci Sports Exerc 37:108-114.

Tosovic D, Ghebremedhin E, Glen C, Gorelick M, Brown JM. 2012. The architecture and contraction time of intrinsic foot muscles. J Electromyogr Kinesiol 22:930-938.

van der Made AD, Wieldraaijer T, Kerkhoffs GM, Kleipool RP, Engebresten L, van Dijk CN, Golano P. 2015. The hamstring muscle complex. Knee Surg Sports Traumatol Arthrosc23:2115-2122.

Verrall GM, Slavotinek JP, Barnes PG, Fon GT, Esterman A. 2006. Assessment of physical examination and magnetic resonance imaging findings of hamstring injury as predictors for recurrent injury. J Orthop Sports PhysTher 36:215-224.

Wickham JB, Brown JM. 1998. Muscles within muscles: the neuromotor control of intra-muscular segments. Eur J Appl Physiol Occup Physiol 78:219-225.

Wickham JB, Brown JM, McAndrew DJ. 2004. Muscles within muscles: anatomical and functional segmentation of selected shoulder joint musculature. J Musculoskelet Res 8:57-73.

Wickiewicz TL, Roy RR, Powell PL, Edgerton VR. 1983. Muscle architecture of the human lower limb. Clin Orthop Relat Res 179:275-283.

Woodley SJ, Mercer SR. 2005. Hamstring muscles: architecture and innervation. Cells Tissues Organs 179:125-141.

Figure Legends:

Figure 1: Ultrasound images of the long head of biceps femoris at 70% of the muscle length. (A)Transverse images were used to measure muscle thickness (arrow) and (B) fascicle length (solid line) and pennation angle (curved-dashed line) were measured using longitudinal images.

Figure 2: An example of fascicle length measurement using digital calipers, taken following dissection and longitudinal sectioning of biceps femoris long head

Table Legends:

Table 1: Mean (SD) architectural measures of BFlh, obtained with ultrasound in healthy male participants (n=19). Abbreviations: ML, muscle length (from origin, excluding free distal tendon); MTJ, musculotendinous junction; SD, standard deviation. *indicates significant difference to all other measurement sites; ^indicates significant difference (P<0.05) to both the most distal (90% ML) and proximal (30% ML) sites.

Table 2: Mean (SD) measures of BFlh architectural data obtained with ultrasound and dissection, cadaver study (n=6). Abbreviations: ICC, Intraclass correlation coefficient; CI, confidence interval; ML, muscle length (from origin, excluding free distal tendon); SD, standard deviation.

Table 3: Comparison of mean (SD) BFlh architectural data obtained using ultrasound from 19 healthy participants and 6 cadaver lower limbs. *indicates significant difference (P<0.05) between corresponding ultrasound measurements. Abbreviations: SD, standard deviation.

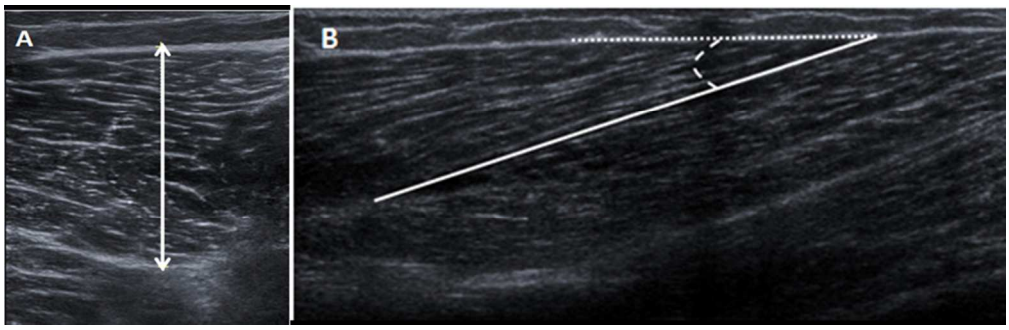

Figure 1: Ultrasound images of the long head of biceps femoris at 70% of the muscle length. (A) Transverse images were used to measure muscle thickness (arrow) and (B) fascicle length (solid line) and pennation angle (curved-dashed line) were measured using longitudinal images.
159x50mm (150 x 150 DPI)

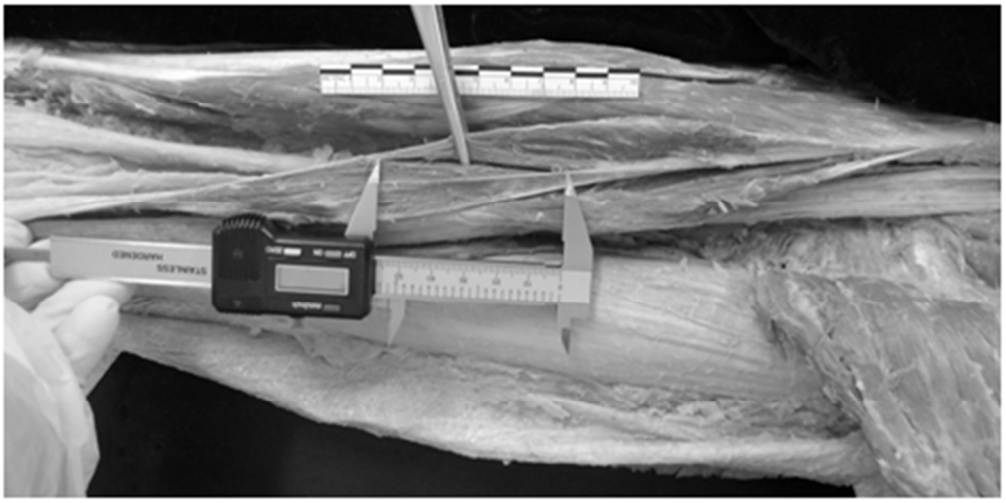

Figure 2: An example of fascicle length measurement using digital calipers, taken following dissection and longitudinal sectioning of biceps femoris long head
131x65mm (150 x 150 DPI)

Architectural parameter	Ultrasound measurement site Mean (SD)				Whole muscle Mean (SD)
	30% ML	50% ML	70% ML	90% ML	
Muscle thickness	27.2 (5.6)	36.4 (5.7)^	34.5 (5.9)^	13.7 (6.5)	27.9 (10.7)
Fascicle length	80.5 (12.0)	82.7 (12.7)	77.6 (13.3)	70.6 (15.1)*	77.9 (14.0)
Pennation angle	10.9 (2.8)*	13.9 (2.8)	14.5 (3.0)	13.5 (2.7)	13.2 (3.1)
Total muscle-tendon length	420.9 (18.1)				
Total muscle length	322.9 (17.2)				
Fascicle length/muscle length ratio	0.25 (0.03)	0.26 (0.04)	0.24 (0.04)	0.22* (0.05)	0.24 (0.04)
Proximal MTJ length (including proximal tendon)	248.3 (17.5)				
Distal MTJ length	160.7 (16.7)				
Distal free tendon length	98.0 (11.5)				

All measurements are in mm except for pennation angle (°) and fascicle length/muscle length ratio

Table 2

Architectural parameter	Method	Measurement site Mean (SD)				Whole muscle Mean (SD)	ICC (95% CI)
		30% ML	50% ML	70% ML	90% ML		
Pennation angle	Ultrasound	9.3 (2.2)	11.5 (3.6)	12.3 (3.8)	9.9 (1.6)	10.7 (3.0)	0.32 (-0.24-0.67)
	Dissection	7.5 (2.6)	8.8 (0.8)	8 (2.3)	7.5 (2.9)	8.0 (2.2)	
Fascicle length	Ultrasound	82.8 (13.7)	80.5 (13.5)	73.3 (17.1)	69.7 (9.3)	76.6 (13.9)	0.82 (0.59-0.92)
	Dissection	88.3 (19.9)	83.5 (20)	79.8 (20.6)	74.3 (20.2)	81.5 (19.5)	
Muscle thickness	Ultrasound	13.4 (3.4)	19.8 (3.5)	18.7 (2.2)	7.6 (0.9)	14.9 (5.6)	0.99 (0.99-0.99)
	Dissection	12.1 (2.9)	18.7 (1.0)	19.8 (1.7)	6.3 (0.7)	14/2 (5.8)	
Total muscle-tendon length	Ultrasound	415.8 (40.5)					0.98 (0.37-0.99)
	Dissection	425.8 (43.6)					
Total muscle length	Ultrasound	297.3 (24.0)					0.84 (-0.18-0.98)
	Dissection	316.7 (34.0)					
Proximal MTJ length	Ultrasound	217.9 (23.3)					0.61 (-0.43-0.95)
	Dissection	217.7 (35.4)					
Distal MTJ length	Ultrasound	129.2 (13.9)					0.36 (-0.42-0.87)
	Dissection	147.5 (12.9)					
Distal free tendon length	Ultrasound	118.5 (19.7)					0.85 (-0.01-0.98)
	Dissection	109.2 (13.6)					

All measurements are in mm except for pennation angle (°)

Architectural parameter	Healthy volunteer Mean (SD)	Cadaver Mean (SD)
Pennation angle	13.2 (3.1)*	10.7 (3.0)
Fascicle length	77.9 (14.0)	76.6 (13.9)
Muscle thickness	27.9 (10.7)*	14.9 (5.6)
Total muscle-tendon length	420.9 (18.1)	415.8 (40.5)
Total muscle length	322.9 (17.1)*	297.3 (24.0)
Proximal MTJ length (including proximal tendon)	248.3 (17.5)*	217.9 (23.3)
Distal MTJ length	160.7 (16.7)*	129.2 (13.9)
Distal free tendon length	98.0 (11.5)	118.5 (19.7)*

All measurements are in mm except for pennation angle (°)